

## Geometrical Frustration in the Spin Liquid $\beta'$ - $\text{Me}_3\text{EtSb}[\text{Pd}(\text{dmit})_2]_2$ and the Valence-Bond Solid $\text{Me}_3\text{EtP}[\text{Pd}(\text{dmit})_2]_2$

E. P. Scriven and B. J. Powell\*

*Centre for Organic Photonics and Electronics, School of Mathematics and Physics, University of Queensland, Brisbane, Queensland 4072, Australia*

(Received 22 August 2011; revised manuscript received 2 April 2012; published 29 August 2012)

We show that the electronic structures of the title compounds predicted by density functional theory are well described by tight binding models. We determine the frustration ratio,  $J'/J$ , of the Heisenberg model on the anisotropic triangular lattice, which describes the spin degrees of freedom in the Mott insulating phase for a range of  $\text{Pd}(\text{dmit})_2$  salts. All of the antiferromagnetic materials studied have  $J'/J \leq 0.5$  or  $J'/J \geq 0.9$ , and all salts with  $0.5 \leq J'/J \leq 0.9$  are known, experimentally, to be charge ordered valence-bond solids or spin liquids.

DOI: [10.1103/PhysRevLett.109.097206](https://doi.org/10.1103/PhysRevLett.109.097206)

PACS numbers: 75.10.Kt, 71.15.Mb, 74.70.Kn, 75.10.Jm

The interplay of geometrical frustration and electronic correlations produces a wide range of exotic phenomena [1,2] in the organic charge transfer salts  $\text{Me}_{4-n}\text{Et}_n\text{Pn}[\text{Pd}(\text{dmit})_2]_2$  (henceforth  $\text{Pn-n}$ ) [3]. At ambient pressure and low temperature, these materials are Mott insulators, many of which are driven superconducting by the application of hydrostatic pressure or uniaxial stress. Most salts display antiferromagnetic (AFM) order, but recent experiments [1,2] suggest that  $\text{Me}_3\text{EtP}[\text{Pd}(\text{dmit})_2]_2$  (P-1) is a valence-bond solid (VBS), and  $\text{Me}_3\text{EtSb}[\text{Pd}(\text{dmit})_2]_2$  (Sb-1) is a type II spin liquid (SL) [2], with a singlet gap but no triplet gap [4].

In this Letter, we report density functional theory (DFT) calculations of the electronic structures of Sb-1 and P-1. We parametrize these results in terms of tight binding models and report the parameters found for a number of  $\text{Pd}(\text{dmit})_2$  salts with AFM or charge ordered (CO) ground states. The simplest model that has been proposed for the insulating phases of the  $\text{Pd}(\text{dmit})_2$  salts is the Heisenberg model on the anisotropic triangular lattice [1,2,5]. In this model, each site represents a  $\text{Pd}(\text{dmit})_2$  dimer,  $J$  is the exchange coupling around the sides of square, and  $J'$  is the exchange interaction along one diagonal. We find that those materials that display long-range AFM order lie in the parameter regimes  $J'/J \leq 0.5$  or  $J'/J \geq 1$  where many-body theories predict long-range magnetic order. Further, all of the materials with CO, SL, or VBS ground states lie in the parameter regime  $0.5 \leq J'/J \leq 0.9$  where the low energy physics remains controversial because there are a number of competing states. We argue that this means that other terms in the Hamiltonian may be crucial for determining the ground state.

The Heisenberg model on the anisotropic triangular lattice has been studied by a range of theoretical methods including linear spin-wave theory [6], series expansions [7], the coupled cluster method [8], large- $N$  expansions [9], variational Monte Carlo calculations [10], resonating valence-bond theory [11–15], pseudofermion functional renormalization group [16], slave rotor theory [17],

renormalization group [18], and the density matrix renormalization group [19]. Collectively, these studies suggest that Néel ( $\pi, \pi$ ) order is realized for  $J'/J \leq 0.5$ , and incommensurate ( $q, q$ ) long-range AFM order is realized for  $J'/J \sim 1$  (in the special case  $J'/J = 1$ , the  $120^\circ$  state with  $q = 2\pi/3$  is realized). However, the ground state for  $0.6 \leq J'/J \leq 0.9$  remains controversial.

Many  $\text{Pd}(\text{dmit})_2$  salts undergo a Mott transition under hydrostatic pressure and/or uniaxial strain [1,2]. Therefore, it is possible that the Heisenberg model misses some essential physics as it represents only the lowest order terms in an expansion in  $t/U$ , where  $t$  is the hopping integral between neighboring sites, and the Hubbard  $U$  is the effective Coulomb repulsion between two electrons on the same site. The next nontrivial term in this expansion introduces ring exchange into the Hamiltonian [2,20]. It has been argued [20], in the context of the SL  $\kappa - (\text{BEDT} - \text{TTF})_2\text{Cu}(\text{CN})_3$  ( $\kappa\text{-CN}$ ), that ring exchange and other higher order terms can drive the breakdown of the  $120^\circ$  order found on the isotropic triangular lattice before  $t/U$  becomes large enough for the Mott transition to occur. Thus, it is clear that the ratio  $t/U$  is vitally important in organic charge transfer salts. This has stimulated several groups to attempt to calculate the  $U$  from first principles. However, different methods give somewhat inconsistent results [21–24], and so the ratio  $t/U$  is not reliably known at present [2]. Nevertheless different methods give reasonably consistent trends in the variation of  $U$  among similar materials. Therefore, we have also investigated the trend in the  $U$  associated with  $[\text{Pd}(\text{dmit})_2]_2$  dimers. We find very little variation of  $U$  across the series, which suggests that ring exchange and other higher-order effects are not primarily responsible for different physics observed in the different  $\text{Pd}(\text{dmit})_2$  salts.

A major impediment to comparing the many-body theories described above to experiment has been the lack of understanding how changing the cation, i.e., choosing  $\text{Pn}$  and  $n$ , changes the parameters in the effective

Hamiltonians of the monomer and dimer models. The only previous parameterizations of the band structures of the  $\text{Pd}(\text{dmit})_2$  salts have come from the extended Hückel model (a parametrized tight-binding model). However, it has been discovered, e.g., from studies of bis(ethylene-dithio)tetrathiafulvalene (BEDT-TTF) salts [21–25], that the extended Hückel model does not provide parameters that are accurate enough for discussions of the subtle effects of quantum frustration, which are at play in both the BEDT-TTF and  $\text{Pd}(\text{dmit})_2$  salts [1,2]. Therefore, we performed DFT band structure calculations in QUANTUM ESPRESSO [26] using the Perdew-Burke-Ernzerhof functional and ultrasoft pseudopotentials with a plane-wave cutoff of 25 Ry and a 250 Ry integration mesh. Crystal structures (Fig. 1) are taken to be those observed by x-ray crystallography [27,28] with only the position of the hydrogen atoms in the cations (which are not visible to x rays) relaxed.

In molecular acceptors, such as  $\text{Pd}(\text{dmit})_2$ , the Hubbard  $U$  associated with a dimer may be written as the sum of two terms  $U = U^{(v)} - \delta U^{(p)}$ , where  $U^{(v)} = E(0) + E(-2) - 2E(-1)$  is the  $U$  of the dimer *in vacuo*,  $E(q)$  is the ground state energy of the dimer with charge  $q$ , and  $\delta U^{(p)}$  is the correction due to the polarizable environment of the molecular solid [24]. We performed DFT calculations  $E(q)$ , and hence  $U^{(v)}$ , in SIESTA [29] using a triplet-zeta plus polarization basis set [24]. However, for solids formed from narrow molecules such as  $\text{Pd}(\text{dmit})_2$  and BEDT-TTF the accurate calculation  $\delta U^{(p)}$  remains an challenging problem [24,30]. Therefore, we report  $U^{(v)}$ , which allows us to understand the trends  $U$  across the systems discussed below.

Although the in-plane crystal and electronic structures of Sb-1 and P-1 are very similar (cf. Fig. 1), there are some subtle differences that should be noted before we discuss our results in detail. Sb-1 takes the bilayer  $\beta'$  phase, found in many  $\text{Pd}(\text{dmit})_2$  salts. In the layer shown molecules stack face-to-face along  $\mathbf{a} - \mathbf{b}$ , but in alternate layers molecules stack in the  $\mathbf{a} + \mathbf{b}$  direction, where  $\mathbf{a}$  and  $\mathbf{b}$  are the crystallographic axes of the conventional unit cell shown in the Fig. 1. The Wigner-Seitz unit cell of Sb-1 is

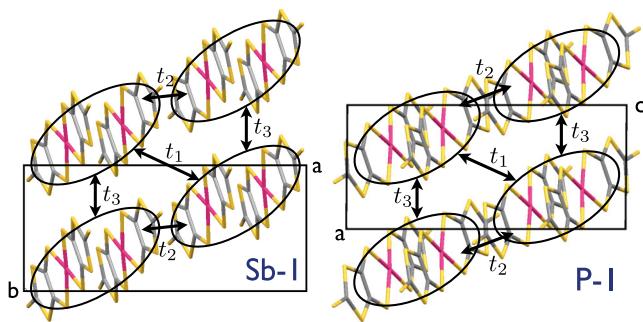


FIG. 1 (color online). In-plane crystal structures and inter-dimer hopping integrals for Sb-1 (left) and P-1 (right). Rings indicate the dimers. The conventional unit cell is marked.

half of this size and therefore only contains one dimer per layer per unit cell. P-1 also forms a bilayer structure; however, in  $\text{Pd}(\text{dmit})_2$  molecules stack along the  $\mathbf{a} + \mathbf{c}$  axes in both layers. Further, in P-1, the conventional and Wigner-Seitz unit cells are identical and contain two dimers per layer per unit cell. Thus, the Wigner-Seitz unit cell of P-1 is approximately twice the size of that of Sb-1 and contains twice as many molecules.

In Fig. 2, we report the calculated band structure of Sb-1. The electronic structure is rather similar to those of N-0 and P-0 [31], which are the only other DFT band structures for salts of  $\text{Pd}(\text{dmit})_2$  that we are aware of. In all three salts, two bands cross the Fermi energy. These bands are derived predominately from the antibonding combination of highest occupied molecular orbitals (HOMOs). It is not immediately obvious that the HOMOs should be partially filled as  $\text{Pd}(\text{dmit})_2$  is electron acceptor, one might expect a partial occupation of the lowest unoccupied molecular orbitals (LUMOs). However, the strong hybridization between the two molecules in each dimer (ringed in Fig. 1) means that the bonding combination of LUMOs is lower in energy than the antibonding combination of HOMOs [2,31]. There are two bands derived predominately from the antibonding combination of HOMOs and two bands derived predominately from the bonding combination of LUMOs because of the two dimers per unit cell.

In Fig. 3, we report the calculated band structure of P-1. There are twice as many bands as there are in Fig. 2 because the Wigner-Seitz unit cell of P-1 contains four dimers rather than two. The charge densities corresponding to the bands that cross the Fermi energy in both Sb-1 and P-1 are reported in the Supplemental Material [32]. We also show fits to the dimer models in Figs. 2 and 3.

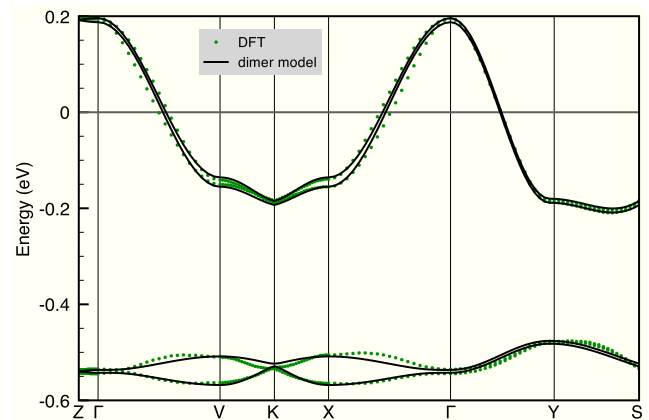


FIG. 2 (color online). Band structure of Sb-1 calculated from DFT (points) and fit to the dimer tight-binding model (curves). The corresponding Fermi surface and the locations of high symmetry points are shown in Fig. 5 of the Supplemental Material [32]. The values of the dimer tight-binding fit (in meV) for the HOMO band are  $t_1 = 37$ ,  $t_2 = 49$ ,  $t_3 = 45$ ,  $t_{\perp} = -2.1$ , and the parameters for the LUMO band are  $t_1 = 7.2$ ,  $t_2 = -15$ ,  $t_3 = -0.2$ ,  $t_{\perp} = -1.5$ .

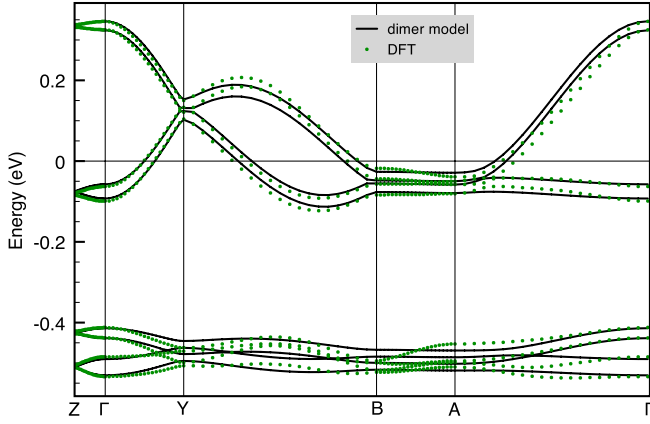


FIG. 3 (color online). Band structure of P-1 calculated from DFT (points) and fit to the dimer tight-binding model (curves). The corresponding Fermi surface and the locations of high symmetry points are shown in Fig. 6 of the Supplemental Material [32]. The values of the dimer tight-binding fit (in meV) for the HOMO band are  $t_1 = 45$ ,  $t_2 = 52$ ,  $t_3 = 52$ ,  $t_{\perp} = 6.7$ ,  $\delta = 16$ , and the fit to the LUMO band yields  $t_1 = 6.6$ ,  $t_2 = -11$ ,  $t_3 = -8$ ,  $t_{\perp} = -8.0$ ,  $\delta = 0$ .

The in-plane tight binding integrals are marked in Fig. 1. Interlayer hopping is described by the hopping integral,  $t_{\perp}$ . For P-1, we also introduce a parameter  $\delta$ , which describes the orbital energy differences in the HOMOs (LUMOs) due to the crystallographically distinct local environments of the two dimers per unit cell per layer. Li *et al.* [33] have argued for a quarter filled model where each site is a single  $\text{Pd}(\text{dmit})_2$  molecule. Fits to the monomer models are reported in the Supplemental Material [32]. Both models provide a good description of the DFT results for both compounds. However, the monomer fit does not appear significantly better than the dimer fit. Therefore, we

conclude that at the level of band structure, the dimer model is sufficient to describe these salts.

In both materials  $t_2 \simeq t_3 > t_1$ . Therefore, in order to make connection with theories of the Heisenberg model on the anisotropic triangular lattice we make the identification  $t = \frac{1}{2}(t_2 + t_3)$ ,  $t' = t_1$ . Thus, we find that  $t'/t = 0.79$  for Sb-1 and  $t'/t = 0.87$  for P-1.  $J'/J = (t'/t)^2$  to leading order in  $t/U$ . This yields  $J'/J = 0.62$  for Sb-1 and  $J'/J = 0.75$  for P-1. Both of these values are in the regime where the ground state of the Heisenberg model remains controversial.

We also calculated the band structures of a range of other salts of  $\text{Pd}(\text{dmit})_2$ . The values of  $J'/J$  determined analogously to those for Sb-1 and P-1 are reported in Table I. Full details of the calculations will be reported elsewhere. We also report our parametrization of the band structure of the  $\kappa - (\text{BEDT} - \text{TTF})_2\text{Cu}(\text{CN})_3$  ( $\kappa\text{-CN}$ ), which has a SL ground state. Note that the value of  $t'/t$  for  $\kappa\text{-CN}$  is in excellent agreement with other estimates from DFT (0.83 [21] and 0.80 [22]). We also report the calculated values of  $U^{(v)}$  for dimers of  $\text{Pd}(\text{dmit})_2$  in each of these systems in Table I. There is no significant variation in  $U^{(v)}$  amongst the  $\text{Pd}(\text{dmit})_2$  salts, and even the BEDT-TTF salt has a remarkably similar  $U^{(v)}$ . The bandwidths  $W$  of salts are also remarkably consistent, cf. the Supplemental Material [32], with the exception of P-2, which has a rather wider band; however, this material displays long-range anti-ferromagnetism. Therefore, we find no evidence that ring exchange is the primary determinant of the magnetic ground state in these materials. This conclusion is supported by experiment. None of the AFM states have been observed to give way to spin-liquid, valence-bond solid, or charge order when pressure is applied to them, which drives the materials towards the Mott transition by decreasing  $U/t$  and, hence, increasing the relative importance of ring exchange [1,2].

TABLE I. Calculated parameters for the anisotropic triangular lattice for a range of  $\text{Me}_{4-n}\text{Et}_n\text{Pn}[\text{Pd}(\text{dmit})_2]_2$  ( $Pn\text{-}n$ ) and  $\kappa - (\text{BEDT} - \text{TTF})_2\text{Cu}(\text{CN})_3$  ( $\kappa\text{-CN}$ ). Where two values are given this indicates the small differences because the two  $t$  hopping integrals are not identical. In the Supplemental Material [32] we also report equivalent results for the local density approximation, which give the same picture as the Perdew-Burke-Ernzerhof results. The column labelled Experiment summarizes the experimentally observed low temperature physics.  $U^{(v)}$  is the calculated effective Coulomb repulsion between two holes on the same dimer *in vacuo*. The variation is small across all of the  $\text{Pd}(\text{dmit})_2$  salts and even between the  $\text{Pd}(\text{dmit})_2$  salts and the BEDT-TTF salt.

Material	Experiment	$t_1$ (meV)	$t_2$ (meV)	$t_3$ (meV)	$t'/t$	$J'/J = (t'/t)^2$	$U^{(v)}$ (eV)
N-3	AFM	54	55	18	0.33–0.33	0.10–0.11	3.13
P-2	AFM	68	50	80	0.62–0.73	0.38–0.53	3.13
Sb-2	CO	33	49	46	0.69–0.75	0.48–0.56	3.18
Sb-1	SL	38	49	46	0.76–0.82	0.58–0.67	3.12
$\kappa\text{-CN}$	SL	43	51	51	0.84	0.71	2.95 [24]
P-1	VBS	45	51	52	0.88–0.89	0.77–0.80	3.12
Cs	CO	42	45	45	0.93	0.87	3.10
Sb-0	AFM	38	51	44	1.17–1.29	1.36–1.66	3.14
As-2	AFM	39	51	43	1.20–1.31	1.44–1.72	3.11

However, note that this comparison of the relative importance of ring exchange across the series does not imply that ring exchange does not play any role in determining the ground state in the region where there are multiple competing ground states, as we will discuss below.

It is clear from Table I that those materials which display long-range magnetic order lie in the parameter ranges  $J'/J \leq 0.5$  or  $J'/J \geq 1$ , while those materials which are found experimentally to have CO, SL, and VBS ground states all lie in the parameter range  $0.5 \leq J'/J \leq 0.9$ . This is precisely the parameter regime where the many-body ground state remains controversial. This suggests that in this parameter regime there are a number of competing ground states, and that other interactions (not included in the anisotropic triangular lattice Heisenberg model) may be important for determining the ground state. Indeed, series expansions calculations [7] find a number of ground states with very similar energies in this parameter regime, supporting our contention. Similarly, the energies of different phases are found to be similar in this regime in coupled cluster calculations [8].

Since we placed this Letter on the arXiv, Hauke [34] has compared the tight binding parameters reported in Table I to his self-consistent spin-wave calculations for the Heisenberg model on the completely anisotropic triangular with three distinct exchange interactions. Taking  $J_2/J_1 = (t_2/t_1)^2$  and  $J_3/J_1 = (t_3/t_1)^2$  he finds that our parameters for the completely anisotropic lattice still predict ground states consistent with those found experimentally.

We therefore conclude that the Heisenberg model gives a clear prediction of when long-range magnetic order will be found in the Pd(dmit)<sub>2</sub> salts. For  $0.5 \geq J'/J$  and  $J'/J \geq 0.9$  the Heisenberg model has a very stable ground state with long-range magnetic order (as witnessed by the good agreement between different quantum many-body theories). Thus, perturbations do not change the nature of the ground state, and long-range order is realized. But, for  $0.5 \leq J'/J \leq 0.9$  there are a number of states that are close in energy (consistent with the disagreement in the ground state predicted by different methods). Thus, other terms in the Hamiltonian, such as intradimer dynamics, ring exchange, elastic forces in the crystal, or the differences in the crystal structures, will play an important role in determining which phases are realized. In this light, it is interesting to note that the LUMO bands are within  $\sim U$  of the HOMO bands, which suggests that they could play an important role. To that end, we report the tight binding fits of these bands in Figs. 2 and 3 and the Supplemental Material [32]. This is in marked contrast from proposals that proximity to a putative quantum critical point is the determining factor in these systems [5,35].

We thank Reizo Kato and Ross McKenzie for helpful discussions. This work was supported by the Australian Research Council under the Discovery (DP1093224) and Queen Elizabeth II (DP0878523) schemes and by an award under the MAS on the NCI-NF.

- \*bjpowell@gmail.com
- [1] K. Kanoda and R. Kato, *Annu. Rev. Condens. Matter Phys.* **2**, 167 (2011).
  - [2] B.J. Powell and R.H. McKenzie, *Rep. Prog. Phys.* **74**, 056501 (2011).
  - [3] Here, Me means methyl, Et means ethyl, *Pn* is a pnictogen, and dmit is 1,3-dithiol-2-thione-4,5-dithiolate.
  - [4] B. Normand, *Contemp. Phys.* **50**, 533 (2009).
  - [5] Y. Shimizu, H. Akimoto, H. Tsujii, A. Tajima, and R. Kato, *J. Phys. Condens. Matter* **19**, 145240 (2007).
  - [6] J. Merino, R.H. McKenzie, J.B. Marston, and C.H. Chung, *J. Phys. Condens. Matter* **11**, 2965 (1999); A.E. Trumper, *Phys. Rev. B* **60**, 2987 (1999).
  - [7] W. Zheng, R.H. McKenzie, and R. R. P. Singh, *Phys. Rev. B* **59**, 14367 (1999); J. O. Fjærestad, W. Zheng, R. R. P. Singh, R. H. McKenzie, and R. Coldea, *Phys. Rev. B* **75**, 174447 (2007).
  - [8] R. F. Bishop, P. H. Y. Li, D. J. J. Farnell, and C. E. Campbell, *Phys. Rev. B* **79**, 174405 (2009).
  - [9] C. H. Chung, J. B. Marston, and R. H. McKenzie, *J. Phys. Condens. Matter* **13**, 5159 (2001).
  - [10] S. Yunoki and S. Sorella, *Phys. Rev. B* **74**, 014408 (2006); D. Heidarian, S. Sorella, and F. Becca, *Phys. Rev. B* **80**, 012404 (2009).
  - [11] B.J. Powell and R.H. McKenzie, *Phys. Rev. Lett.* **98**, 027005 (2007).
  - [12] B.J. Powell and R.H. McKenzie, *Phys. Rev. Lett.* **94**, 047004 (2005).
  - [13] J. Y. Gan, Y. Chen, Z. B. Su, and F. C. Zhang, *Phys. Rev. Lett.* **94**, 067005 (2005).
  - [14] J. Liu, J. Schmalian, and N. Trivedi, *Phys. Rev. Lett.* **94**, 127003 (2005).
  - [15] Y. Hayashi and M. Ogata, *J. Phys. Soc. Jpn.* **76**, 053705 (2007).
  - [16] J. Reuther and R. Thomale, *Phys. Rev. B* **83**, 024402 (2011).
  - [17] J.G. Rau and H.-Y. Kee, *Phys. Rev. Lett.* **106**, 056405 (2011).
  - [18] O. A. Starykh and L. Balents, *Phys. Rev. Lett.* **98**, 077205 (2007).
  - [19] M. Q. Weng, D. N. Sheng, Z. Y. Weng, and R. J. Bursill, *Phys. Rev. B* **74**, 012407 (2006); D. N. Sheng, O. I. Motrunich, and M. P. A. Fisher, *ibid.* **79**, 205112 (2009); A. Weichselbaum and S. R. White, *ibid.* **84**, 245130 (2011).
  - [20] O. I. Motrunich, *Phys. Rev. B* **72**, 045105 (2005); **73**, 155115 (2006); H. Y. Yang, A. M. Lauchli, F. Mila, and K. P. Schmidt, *Phys. Rev. Lett.* **105**, 267204 (2010).
  - [21] H. C. Kandpal, I. Opahle, Y.-Z. Zhang, H. O. Jeschke, and R. Valentí, *Phys. Rev. Lett.* **103**, 067004 (2009).
  - [22] K. Nakamura, Y. Yoshimoto, T. Kosugi, R. Arita, and M. Imada, *J. Phys. Soc. Jpn.* **78**, 083710 (2009).
  - [23] E. Scriven and B. J. Powell, *J. Chem. Phys.* **130**, 104508 (2009).
  - [24] E. Scriven and B. J. Powell, *Phys. Rev. B* **80**, 205107 (2009).
  - [25] F. L. Pratt, *Physica (Amsterdam)* **405B**, S205 (2010).
  - [26] P. Giannozzi *et al.*, *J. Phys. Condens. Matter* **21**, 395502 (2009).

- [27] R. Kato, A. Tajima, A. Nakao, and M. Tamura, *J. Am. Chem. Soc.* **128**, 10016 (2006).
- [28] R. Kato (private communication).
- [29] J. M. Soler, E. Artacho, J. D. Gale, A. García, J. Junquera, P. Ordejón, and D. Sánchez-Portal, *J. Phys. Condens. Matter* **14**, 2745 (2002).
- [30] L. Cano-Cortes, A. Dolfen, J. Merino, and E. Koch, *Physica (Amsterdam)* **405B**, S185 (2010).
- [31] T. Miyazaki and T. Ohno, *Phys. Rev. B* **59**, R5269 (1999); **68**, 035116 (2003).
- [32] See Supplemental Material at <http://link.aps.org/supplemental/10.1103/PhysRevLett.109.097206> for a description of and fits to the monomer model, LDA band structures, Fermi surfaces, and electron density plots and movies.
- [33] H. Li, R. T. Clay, and S. Mazumdar, *J. Phys. Condens. Matter* **22**, 272201 (2010).
- [34] P. Hauke, [arXiv:1205.1955](https://arxiv.org/abs/1205.1955).
- [35] For a review, see S. Sachdev, [arXiv:0901.4103](https://arxiv.org/abs/0901.4103).